Super twisting sliding mode control algorithm of a discharge lamp for water sterilization

Aicha Aissa Bokhtache, Abdallah Zegaoui, Rachid Taleb, Michel Aillerie

ISSN: 04532198
Volume 62, Issue 04, April, 2020

Super twisting sliding mode control algorithm of a discharge lamp for water sterilization

Aicha AISSA BOKHTACHE[1*, 2], Abdallah ZEGAOUI[1, 2], Rachid TALEB[1], Michel AILLERIE[2]

Electrical Engineering Department, Hassiba Benbouali University, Chlef, Algeria
Laboratoire Génie Electrique et Energies Renouvelables (LGEER)[1]
Laboratoire Matériaux Optiques, Photonique et Systèmes, University of Lorraine, Metz, France[2]

Abstract— Electronic ballasts allow to the discharge lamps to improve the quality of radiation by operating at high frequency. In this work, the design of a high-frequency power supply is proposed (multicellular converter series 4-cell based electronic ballast) to supply a low-pressure mercury-argon Ultraviolet-C (UVC) lamp for sterilization with a sinusoidal current of 50 kHz frequency and an effective value of 0.65A to have a germicidal effect for water purification (a maximum of UV radiation at 253.7 nm). The objective is the elaboration of modern control laws for a discharge lamp powered by a series multicellular converter for water sterilization. The control that we have used is the higher order sliding modes "super twisting algorithm", and for the converter, we have adopted the direct control. The performance evaluation of the proposed regulators was carried out by conducting several closed loop robustness tests.

Keywords— Sterilization, Discharge lamp, Electronic ballast, Sliding mode control, Super twisting algorithm, Direct control, UVC.

1. Introduction

The theory of sliding-mode control was born about fifty years ago as a result of Utkin's work but these early algorithms did not generate an ideal sliding regime and could therefore create local instability (Chattering) [1], [2], [3]. Twenty years later, Emel'yanov took over the old works (first sliding modes) and modified them (higher order sliding modes) keeping all the advantages and removing this phenomenon of instability while by increasing the precision [4], [5]. The super-twisting algorithm only applies to the class of systems with a relative degree equal to one in relation to the sliding variable. Consequently, the discontinuity acts on the first derivative of the control input u, this end becomes a continuous function, allows for avoiding the chattering phenomenon. Unlike the twisting algorithm, this algorithm does not require no information on the derivative of S (hence its practical interest) while maintaining good robustness properties [6], [7].

2. Direct control of serial multicellular converters

The system used consists of a five levels multicellular inverter (four switch cells in series), supplying a discharge lamp for the sterilization of water as shown in Figure 1. The characteristics of the lamp-ballast system are given in the references [8], [9]. We have considered in our application a lamp manufacturing by Philips®, powered at 65W designed for water treatment at ambient temperature with an emitted light at 253.7nm [10], [11]. The various parameters of the lamp, as extracted from the datasheet are summarized in Table 1 [9], [12].

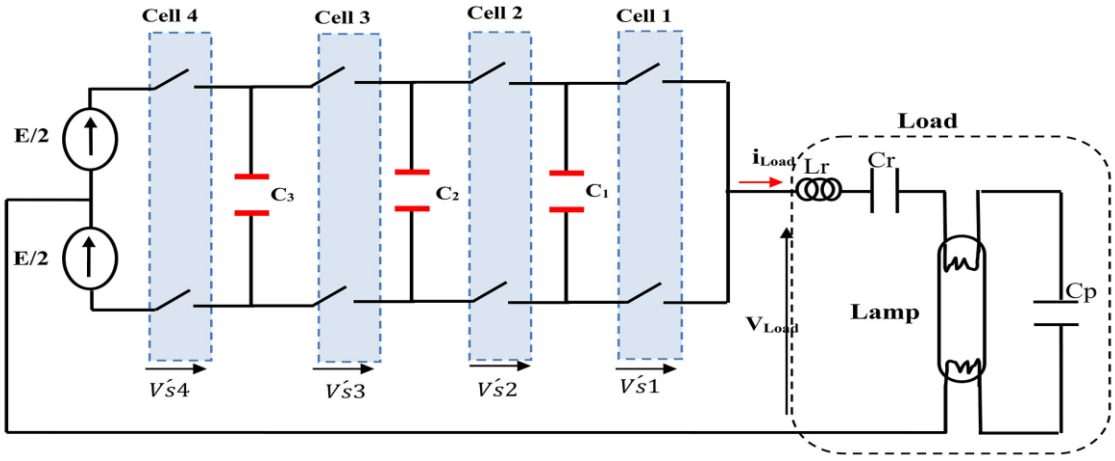

Figure 1. Five levels multicellular inverter (four switch cells in series)

Table 1. Electronic ballast circuit parameters

r_f	F	R_{arc}	L_F	C_F	L_r	C_r	C_p
5Ω	50KHz	170.769 Ω	1.5mH	220nF, 630V	1.3mH	10 nF/630V	4.7nF/1600V

The transfer function of the system is given by [9], [12], [13]. As a result, the transfer function of the open loop system is:

$$\frac{I_{load}}{V_{load}} = \frac{(R_{arc}+rf)C_rC_ps^2+C_rs}{(R_{arc}+rf)L_rC_rC_ps^3[(2R_{arc}+rf)L_rC_rC_p+L_rC_r]s^2+(R_{arc}+rf)(C_r+C_p)s+1} \quad (1)$$

We express the transfer function of the system with respect to the arc current of the I_{arc} lamp in order to regulate this current further. By applying the current divider theorem, will result in:

$$I_{arc}(s) = \frac{\frac{1}{C_ps}+rf}{R_{arc}+rf+\frac{1}{C_ps}}.I_{load}(s) \quad (2)$$

$$I_{arc}(s) = \frac{rf.C_ps+1}{(R_{arc}+rf)C_ps+1}.I_{load}(s) \quad (3)$$

Consequently, the current of the lamp $I_{load}(s)$ is:

$$I_{load}(s) = \frac{(R_{arc}+rf)C_ps+1}{rf.C_ps+1}.I_{arc}(s) \quad (4)$$

By injecting equation (1) into (4), we will have the following transfer function:

$$\frac{I_{arc}}{V_{load}} = \frac{rfC_rC_ps^2+C_rs}{(R_{arc}+rf)L_rC_rC_ps^3[(2R_{arc}+rf)L_rC_rC_p+L_rC_r]s^2+(R_{arc}+rf)(C_r+C_p)s+1} \quad (5)$$

The objective of the direct is doubled. On the one side, it must ensure the voltages across the floating capacitors at their reference values, both static and dynamic. On the other side, the discrete level of voltage

required at the output of the converter must be ensured also. Thus, the control algorithm will choose the state of the switch cells of the converter based on [1], [9]:

- The knowledge of the discrete level of voltage required. The output voltage can take (p + 1) values whose ideal amplitude of each level is given by:

$$V_j = j * \frac{E}{p}, j = 0, 1, \dots p \quad (6)$$

where V_j represents the discrete level j of voltage and p is the number of cells.

- The knowledge of the state of the voltages at the terminals of the floating capacitors with respect to its equilibrium value. The voltage across each floating capacitor can take three states:
  a) When its voltage level is in an allowable band, around its equilibrium value. It's the state of equilibrium.
  b) When its voltage level is above the allowable band. This is the state of higher imbalance.
  c) When its voltage level is below the allowable band. This is the state of lower imbalance.

Table 2 gives the theoretical output voltage V_{ch}, charging or discharging capacitors (C_1, C_2, C_3) according to the control of the switches (u_1, u_2, u_3, u_4) and the direction of the current (+I, -I).

Table 2. Output voltage level with corresponding conducting switches

Output voltage					Switch control				Balancing capacitors						N°
V_{ch}					u_1	u_2	u_3	u_4	C_1		C_2		C_3		
-E/2	-E/4	0	E/4	E/2					+I	-I	+I	-I	+I	-I	
x					0	0	0	0	0	0	0	0	0	0	1
	x				0	0	0	1	0	0	0	0	+	−	2
	x				0	0	1	0	0	0	+	−	−	+	3
		x			0	0	1	1	0	0	+	−	0	0	4
	x				0	1	0	0	+	−	−	+	0	0	5
		x			0	1	0	1	+	−	−	+	+	−	6
		x			0	1	1	0	+	−	0	0	−	+	7
			x		0	1	1	1	+	−	0	0	0	0	8
	x				1	0	0	0	−	+	0	0	0	0	9
		x			1	0	0	1	−	+	0	0	+	−	10
		x			1	0	1	0	−	+	+	−	−	+	11
			x		1	0	1	1	−	+	+	−	0	0	12
		x			1	1	0	0	0	0	−	+	0	0	13
			x		1	1	0	1	0	0	−	+	+	−	14
			x		1	1	1	0	0	0	0	0	−	+	15
				x	1	1	1	1	0	0	0	0	0	0	16

In the columns concerning the balancing of the capacitors, the 0 mean an unused capacitor, the (+) correspond to an increase in the charge of the capacitors while the (-) interpret a diminution. In this Table we can establish a control law to maintain the balancing of the capacitors by considering that the current is constant over a switching period. As we can also see, if we want to generate a voltage of -*E*/2 or *E*/2 the capacitors are not solicited. In contrast if we want to produce a voltage of -*E*/4 or *E*/4 to keep the balancing of the capacitors it will be necessary to use four different control cycles. Similarly, to generate a zero voltage, we will have to use at least two cycles in order to maintain the balancing of the capacitors. As we can see in Table 2, this converter can generate five different voltage levels. For better accuracy when controlling discharge lamp we can generate seventeen voltage values, from the five reference voltages by applying four voltage levels during one switching period. In Figure 2, the voltages can be generated from the five basic levels (top) and the voltage thresholds (bottom) to generate the control of switches.

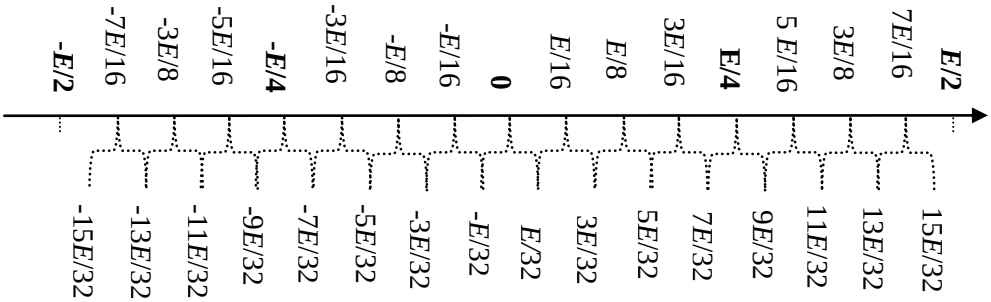

Figure 2. Diagram of the voltages to generate

To increase the control accuracy of the arc current, it is necessary to generate other intermediate levels whose average value over a switching period is equal to the value of the desired voltage at the output of the converter. The number of intermediate levels is arbitrary; in our case we have chosen seventeen levels of tension. To generate the seventeen possible voltage values, we divided the splitting period into four. In addition, knowing that it takes at least four control cycles to keep condenser balancing, we have further subdivided by four the converter chopping period. We generated the algorithm logically, to keep the capacitors balanced while limiting the number of switches. Table 3 shows, for example, the control of the switches to generate the voltage 3*E*/16 for *I* positive or negative, we successively apply sixteen controls during a converter chopping period (Figure 3). Table 4 present the seventeen voltage values.

Table 3. Generation of tension 3*E*/16

	P_1	P_2	P_3	P_4	P_5	P_6	P_7	P_8	P_9	P_{10}	P_{11}	P_{12}	P_{13}	P_{14}	P_{15}	P_{16}
u_1	1	1	1	1	1	1	1	1	1	1	1	0	0	0	0	0
u_2	1	1	1	1	1	1	1	1	0	0	0	0	0	1	1	1
u_3	1	1	1	0	0	0	0	0	1	1	1	1	1	1	1	1
u_4	0	0	0	0	0	1	1	1	1	1	1	1	1	1	1	1
N°	15	15	15	13	13	14	14	14	12	12	12	4	4	8	8	8

ISSN: 04532198
Volume 62, Issue 04, April, 2020

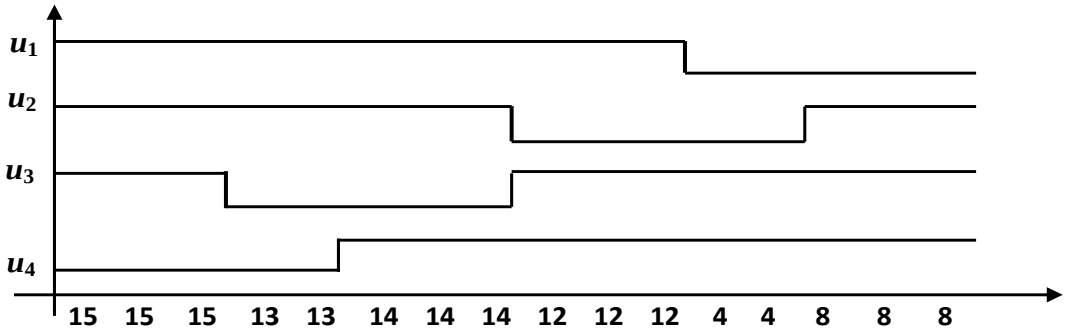

Figure 3. Switching states for generation of tension 3*E*/16

Table 4. Generation of seventeen voltage values

N°	P_1	P_2	P_3	P_4	P_5	P_6	P_7	P_8	P_9	P_{10}	P_{11}	P_{12}	P_{13}	P_{14}	P_{15}	P_{16}
E/2	16	16	16	16	16	16	16	16	16	16	16	16	16	16	16	16
7*E*/16	16	15	16	16	16	14	16	16	16	12	16	16	16	8	16	16
3*E*/8	16	16	15	15	16	16	14	14	16	16	12	12	16	16	8	8
5*E*/16	16	15	15	15	16	14	14	14	16	12	12	12	16	8	8	8
E/4	15	15	15	15	14	14	14	14	12	12	12	12	8	8	8	8
3*E*/16	15	15	15	13	13	14	14	14	12	12	12	4	4	8	8	8
E/8	15	15	11	11	11	11	12	12	8	8	6	6	6	6	14	14
E/16	15	13	13	13	14	6	6	6	8	4	4	4	12	11	11	11
0	13	13	13	13	10	10	10	10	4	4	4	4	7	8	8	8
-*E*/16	2	4	4	4	3	11	11	11	9	13	13	13	5	6	6	6
−*E*/8	2	2	6	6	6	6	5	5	9	9	11	11	11	11	3	3
−3*E*/16	2	2	2	4	4	3	3	3	5	5	5	13	13	9	9	9
−*E*/4	2	2	2	2	3	3	3	3	5	5	5	5	9	9	9	9
−5*E*/16	1	2	2	2	1	3	3	3	1	5	5	5	1	9	9	9
−3*E*/8	1	1	2	2	1	1	3	3	1	1	5	5	1	1	9	9
−7*E*/16	1	2	1	1	1	3	1	1	1	5	1	1	1	9	1	1
−*E*/2	1	1	1	1	1	1	1	1	1	1	1	1	1	1	1	1

3. Super twisting sliding mode control of a discharge lamp

This method generalizes the essential sliding mode idea by acting on the higher order time derivatives of the sliding manifold, instead of influencing the first time derivative as it is the case in Sliding Mode Control (SMC), therefore reducing chattering and avoiding strong mechanical efforts while preserving SMC advantages. In order to ensure the i_{arc} convergence to their reference, a Super Twisting Sliding Mode Control (STSMC) is used [14], [15], [16]. We will define by the error between the reference arc current and the arc current of the lamp:

$$e = i_{arc} - i_{arcref} \tag{7}$$

We choose the sliding surface *S* as follows:

$$S = e(t) = i_{arc} - i_{arcref} \tag{8}$$

We derive a first time:

$$\dot{S} = \dot{\iota_{arc}} - \dot{\iota_{arcref}} \quad (9)$$

We express $\dot{S}$ according to the system parameters:

$$\dot{S} = \frac{1}{(R_{arc}+r_f)*C_p}(r_f * C_p * (\dot{i_l}) + i_l - i_{arc}) - (\dot{\iota_{arcref}}) \quad (10)$$

with:

$$(\dot{\iota_l}) = \frac{1}{L_r}(u - \frac{1}{C_r}\int i_l dt - r_f * i_l - R_{arc} * i_{arc}) \quad (11)$$

then:

$$\dot{S} = \frac{r_f}{L_r(R_{arc}+r_f)} * u + g(t) \quad (12)$$

with:

$$g(t) = \frac{1}{L_r(R_{arc}+r_f)*C_p}(r_f * C_p * (-\frac{1}{C_r}\int i_l dt - r_f * i_l - R_{arc} * i_{arc}) + i_l - i_{arc}) - (\dot{\iota_{arcref}}) \quad (13)$$

$$\ddot{S} = \frac{r_f}{(R_{arc}+r_f)} * \dot{u} + \dot{g}(t) \quad (14)$$

by identification of equation (14) with equations of super twisting algorithm [17] we find:

$$|\dot{g}(t)| \leq \emptyset \quad (15)$$

$$|K_m| \leq \frac{r_f}{L_r(R_{arc}+r_f)} \quad (16)$$

where ϕ and K_m are positive constants.

We must reduce $|\dot{g}(t)|$ i.e. ϕ to determine the parameters α and β of super twisting algorithm [17].

with:

$$\alpha \geq \frac{\emptyset}{K_m} \quad (17)$$

$$0 < \beta \leq 0.5 \quad (18)$$

4. Simulation results

To ensure a good efficiency of the radiation discharge lamp, we must keep the arc current of the lamp strictly stable around a constant value close to 0.65A. We must therefore impose a regulation of the arc

ISSN: 04532198
Volume 62, Issue 04, April, 2020

current with a reference of 0.65A. The difference will be transformed into switching frequency of the switches.

4.1 Load voltage and flying capacitor voltages

In Figure 4, the output voltage of the converter follows its intermediate values (-*E*/2, -*E*/4, 0, *E*/4, *E*/2), with a THD (Total Harmonic Distortion) of 7.83%, only after a delay which is due to the delay of stabilization of the voltages at the terminals of the floating capacitors (Figure 5) with the values *j***E*/*P* corresponding to V_{C1} = 200V, V_{C2} = 400V and V_{C3} = 600V.

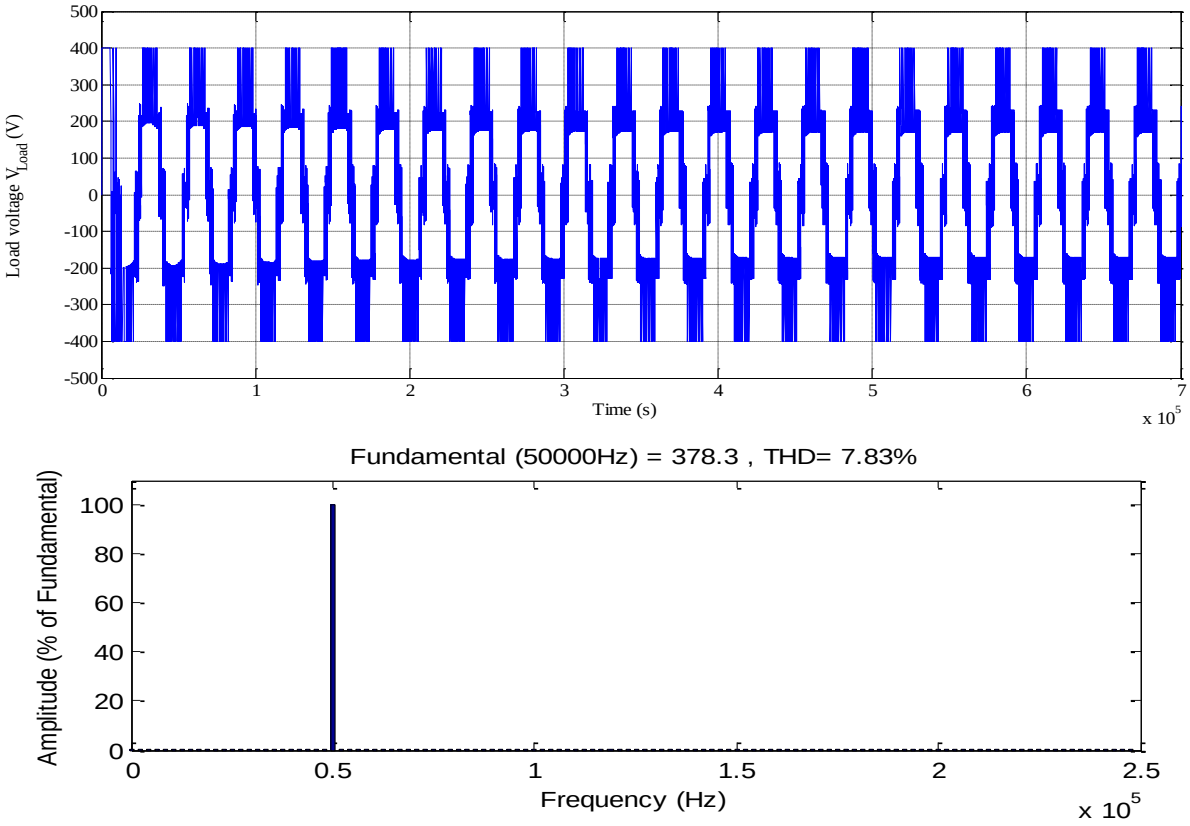

Figure 4. Waveform and THD of the load voltage with super twisting sliding mode control

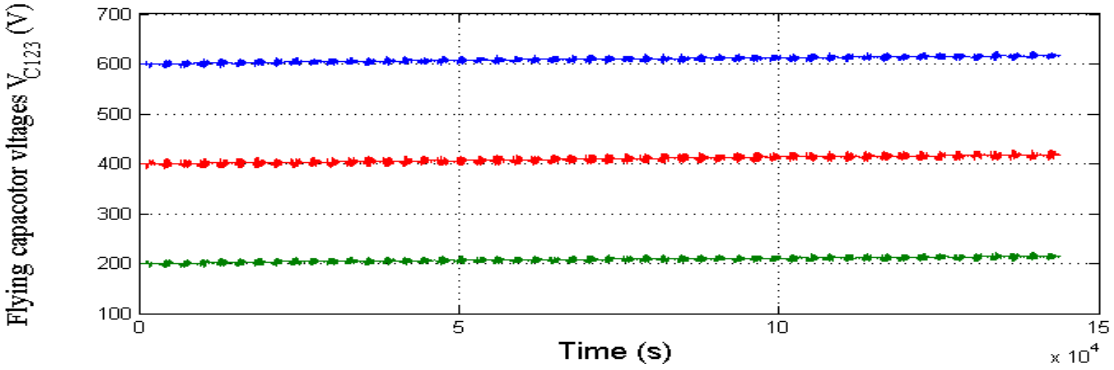

Figure 5. Flying capacitor voltages with super twisting sliding mode control

4.2 Load current

Due to the high voltage's stability of floating capacitors, we see that the load current shown in Figure 6, is sinusoidal with a frequency of 50kHz and a THD of 0.23%.

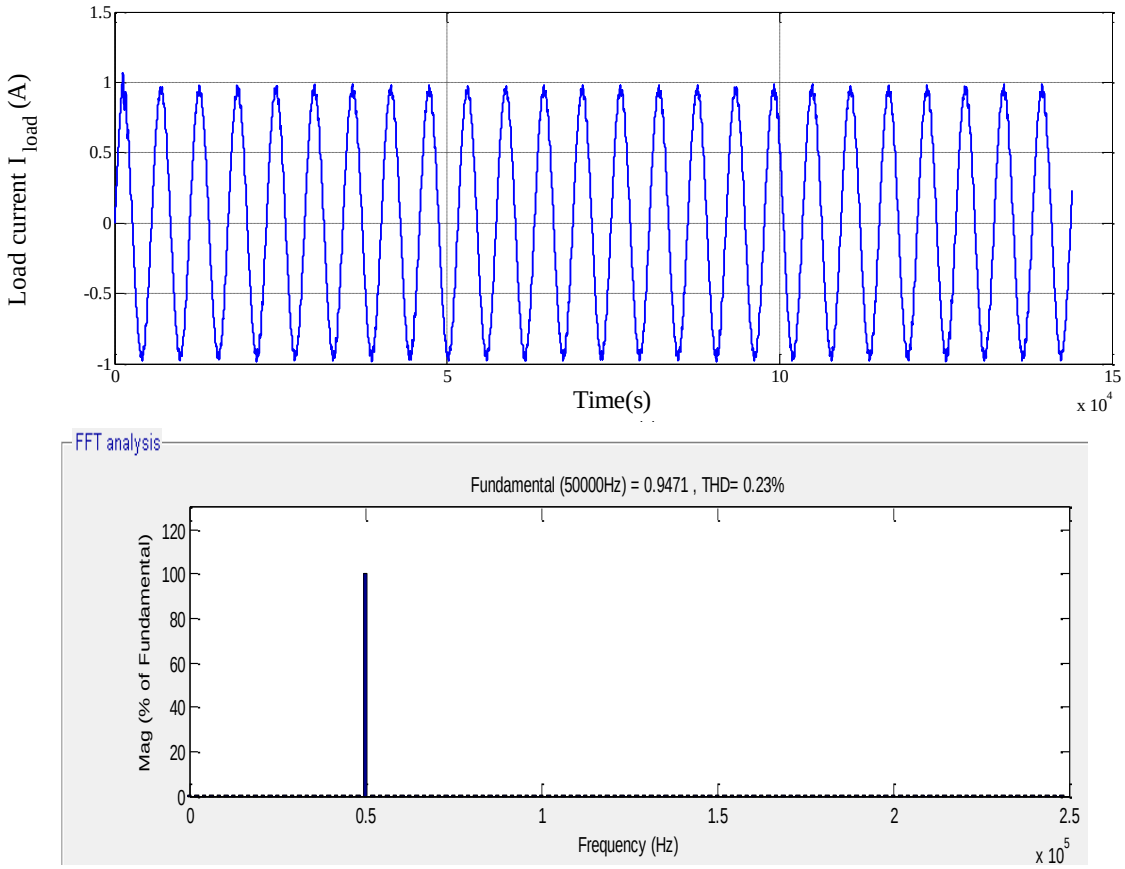

Figure 6. Waveform and THD of the load current with super twisting sliding mode control

4.3 Arc voltage, arc current and effective arc current

According to the Figures 7 and 8 the waveforms of the arc voltage and current are sinusoidal, and their frequencies are identical to the frequency of the modulator (50kHz) with a THD of 0.12% for both, that means they are in phase (which explains that the discharge lamp behaves like a resistance in arc regime). Note also on the Figure 9 that the effective value of current arc reaches the desired value which is 0.65A at the end of 70µs with an accuracy of 0.001A.

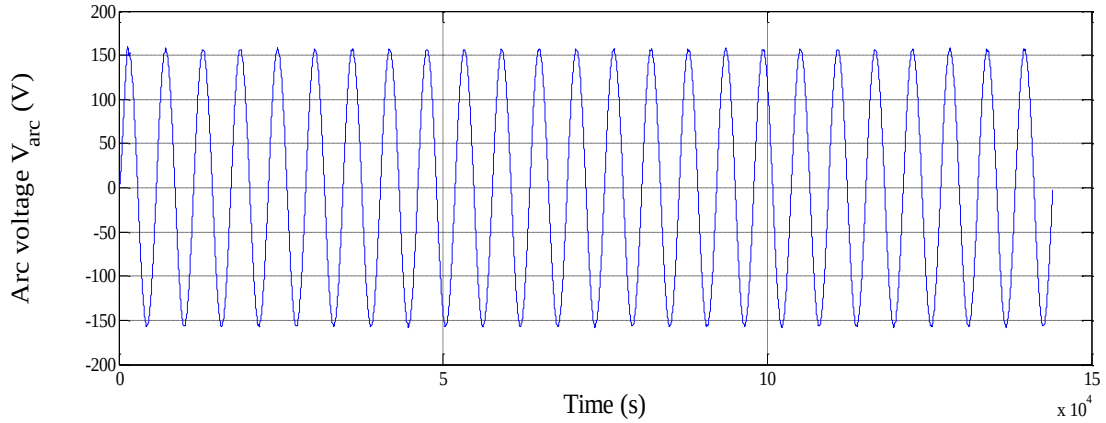

ISSN: 04532198
Volume 62, Issue 04, April, 2020

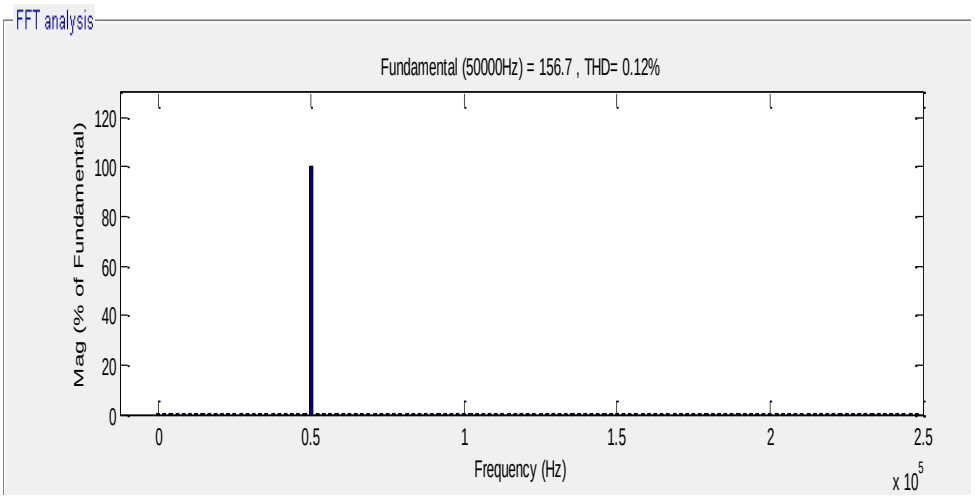

Figure 7. Waveform and THD of the arc voltage with super twisting sliding mode control

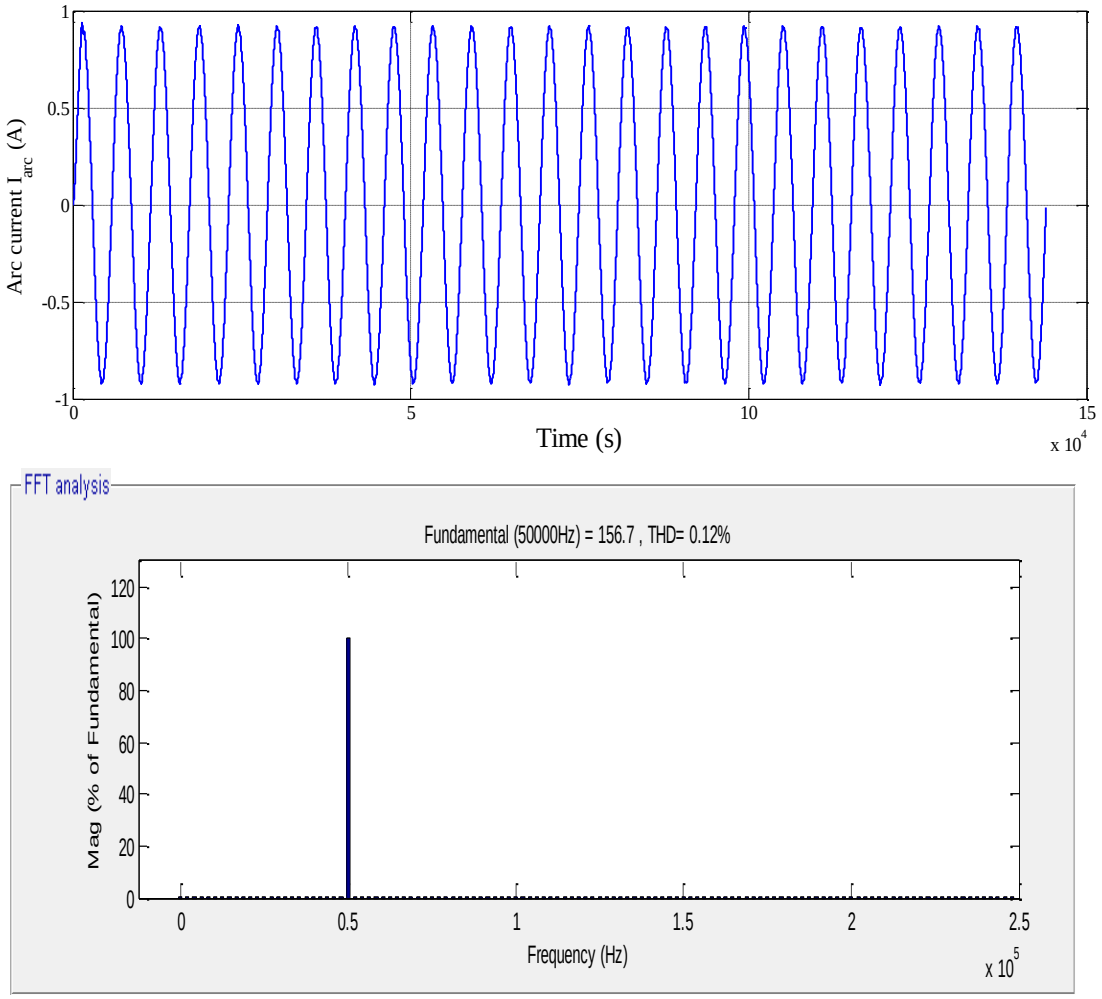

Figure 8. Waveform and THD of the arc current with super twisting sliding mode control

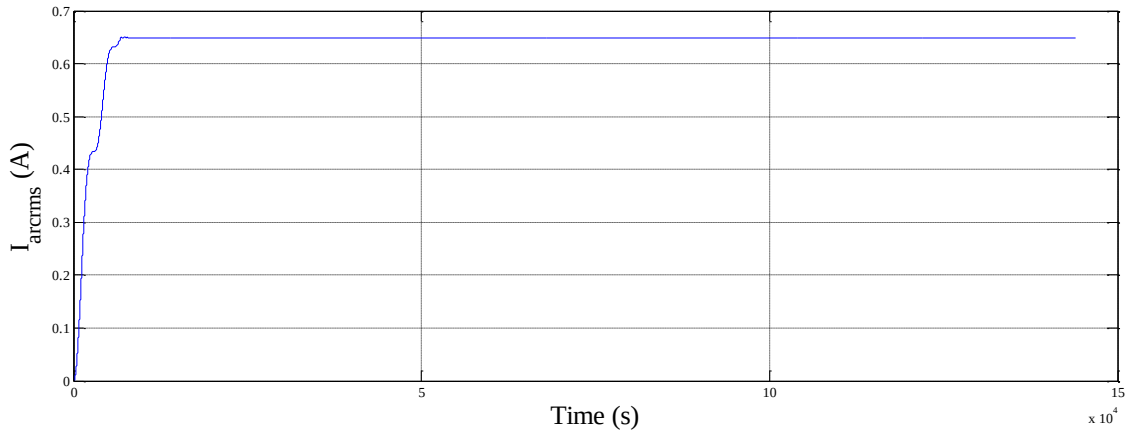

Figure 9. Effective arc current with super twisting sliding mode control

5. Conclusion

The obtained performances obtained in this work with the five levels multicellular inverter used for supply a discharge lamp for water sterilization based super twisting sliding mode control, prove that the waveforms of current and voltage are closer to the sine wave (THD equal to 0.12% for both arc lamp current and arc lamp voltage) with frequency of 50kHz. The results were in complete agreement with our targets.

6. References

[1] V. Utkin, J. Shi, "Integral sliding mode in systems operating under uncertainty conditions", Proceedings of 35th IEEE Conference on Decision and Control, vol. 4, pp. 4591-4596, Kobe, Japan, 1996.

[2] V. Utkin, J. Guldner, J. Shi. "Sliding mode control in electro-mechanical systems", CRC press, 2017.

[3] V. Utkin, "Sliding mode control design principles and applications to electric drives", in IEEE Transactions on Industrial Electronics, vol. 40, no. 1, pp. 23-36, Feb. 1993.

[4] S. V. Emel'yanov, S. K. Korovin, A. Levant, "High-order sliding modes in control systems", Computational Mathematics and Modeling, vol. 7, no. 3, pp. 294-318, 1996.

[5] S. V. Emel'yanov, "Theory of variable-structure control systems: Inception and initial development", Computational Mathematics and Modeling, vol. 18, no. 4, pp. 321-331, 2007.

[6] A. Swikir, V. Utkin, "Chattering analysis of conventional and super twisting sliding mode control algorithm", 14th International Workshop on Variable Structure Systems (VSS), pp. 98-102, Nanjing, 2016.

[7] Z. Li, M. Ruan, H. Wang, S. Zhang, "Chaos Control of Boost Converter Based on Super-Twisting Sliding Mode Control", Chinese Control and Decision Conference (CCDC), pp. 188-193, Nanchang, China, 2019.

[8] A. Aissa Bokhtache, "Commande d'un système lampe à décharge-ballast électronique pour épuration des eaux", Magister Thesis, Hassiba Benbouali University, Chlef, Algeria, 2005.

[9] A. Aissa Bokhtache, “Contribution à la commande d’un système lampe à décharge-ballast électronique pour épuration des eaux”, PhD Thesis, National Polytechnic School, Algiers, Algeria, 2017.

[10] A. Aissa Bokhtache, A. Zegaoui, B. Belmadani, M.S. Boucherit, “Water Purification by a Discharge Lamp-Electronic Ballast System Using a Full Bridge Inverter”, Energy Procedia, vol. 74, pp. 446-452, August 2015.

[11] A. Aissa Bokhtache, A. Zegaoui, M. Aillerie, A. Djahbar, H. Allouache, K. Hemici, F.Z. Kessassia, M.S. Boucherit, “Power Supply Improvements for ballasts-low pressure mercury/argon discharge lamp for water purification”, AIP Conference Proceedings 1814, 2017.

[12] A. Aissa Bokhtache, A. Zegaoui, M. Kellal, M.S. Boucherit, B. Belmadani, M. Aillerie, “Optimization based on fuzzy logic control of discharge lamp-electronic ballast system for water purification”, Electric Power Components and Systems, vol. 44, pp. 1981-1990, 2016.

[13] A. Aissa Bokhtache, A. Zegaoui, M. Aillerie, A. Djahbar, K. Hemici, “Development and optimization of a matrix converter supplying an electronic ballast-UV lamp system for sterilization”, International Conference on Technologies and Materials for Renewable Energy, Environment and Sustainability (TMREES’18), Lebanon 2018.

[14] C. Yi-mei, L. Yong-chao, L. Kang-li, “Sliding mode Control for Quad-rotor Based on Super-twisting Algorithm Disturbance Observation and Compensation”, Chinese Control And Decision Conference (CCDC), pp. 3123-3128, Nanchang, China, 2019.

[15] M. E. Azzaoui, H. Mahmoudi, K. Boudaraia, C. Ed-dahmani, “FPGA implementation of super twisting sliding mode control of the doubly fed induction generator”, 14th International Multi-Conference on Systems, Signals & Devices (SSD), pp. 649-654, Marrakech, 2017.

[16] B. Brogliato, A. Polyakov, D. Efimov, “The implicit discretization of the super-twisting sliding-mode control algorithm”, 15th International Workshop on Variable Structure Systems (VSS), pp. 349-353, Graz, 2018.

[17] H. Kahal, R. Taleb, Z. Boudjema, A. Bouyekni, “Super Twisting Sliding Mode Control of Dual Star Induction Generator for Wind Turbine”, The Mediterranean Journal of Measurement and Control, vol. 13, no. 03, pp. 788 - 794, 2017.